

Optimal Deep Convolutional Neural Network based Fusion Model for Soil Nutrient Analysis

Sharmila.G¹, Kavitha Rajamohan²

Department of Computer Science ,CHRIST (Deemed to be University),Bengaluru , India
sharmila.g@res.christuniversity.in

Department of Computer Science,CHRIST (Deemed to be University),Bengaluru , India
kavitha.r@christuniversity.in

Abstract—The vast majority of people in India, agriculture is their main line of work, and it has a large economic impact.. Soil is important for supplying vital nutrients to crops for better yield. Determining soil nutrients is certainly essential for selecting appropriate crops and monitoring growth. Common methods used by agriculturalists are inadequate to satisfy increasing demands and have to obstruct cultivating soil. For a better crop yield, agriculturalists must have an awareness regarding the soil nutrients for a specific crop. There comes a need for using Deep learning methods in soil analysis that would help farmers in the domain. This study introduces an Optimal Deep Convolutional Neural Network Fusion Model for Soil nutrient Type Classification (ODCNNF-STC) technique. The presented ODCNNF-STC technique examines the input soil images to classify them into different nutrients present in the soil. In this approach, the noise present in the soil images are initially filtered using a bilateral filter (BF) followed by contrast enhancement. The preprocessed soil images are fed to the model formed by the fusion of DenseNet201 and InceptionResNetV2 models extracting the soil images that can successfully differentiate soil nutrients. Finally, classification of soil nutrients were performed by three classifiers namely extreme learning machine (ELM), RMSProp optimizer-based 1DCNN, and RMSProp optimizer-based Stacked Auto Encoder (SAE). The experimental validation of ODCNNF-STC method is examined on real-time dataset of soil images with a maximum accuracy of 99.39% over recent methods.

Keywords- Soil type analysis; Image processing; RMSProp optimizer; Deep learning; Fusion model; Computer vision

I. INTRODUCTION

In India, the majority of the population depends on agriculture as a primary occupation and source of income, thus the demand for production increases exponentially. Nevertheless, with industrial development, the number of farmlands was drastically reduced [1]. Data like the usage of pesticides, fertilizers, soil, and meteorological data should be made available to the agriculturalists in a prompt and precise manner to make accurate decisions depending on the types of crops that have to be planted and to attain a good yield [2]. Farmers by analyzing the suitable conditions, thereby minimizing the loss and damage of crops that occur because of adverse conditions, can realize better crop production. Several hybrid varieties of plants are produced every day [3]. Yet, while compared to naturally produced crops, hybrid varieties lack vital nutrients. The artificial techniques spoil soil quality and cause environmental depletion. Loss prevention is the main target of these artificial methods [4]. But crop losses are diminished and productivity can be augmented by the farmers only with precise knowledge of different factors. One of the main factors to maintain a sustainable crop productivity level is soil fertility management [5]. This guarantees that the soil has the potential to provide the necessary nutrients to the plants in

the appropriate time and right amount, in the available form. The presence or absence of macro and micronutrients aids in ascertaining the fertility level of the soil. Throughout the plant life cycle, the micronutrients are decisive. Crop failure occurs in case of abnormal plant growth if there is a micronutrient deficiency in the soil.

Deep learning (DL) and machine learning (ML) models are currently implemented with models of soil-based classifier approaches [6]. Different ML approaches are used to forecast soil types, soil moisture, and soil nutrient content. Soil fertility indices along with 20 methods that include SVM, bagging, AdaBoost, and NN, RF, were used for categorizing soil nutrient levels and labeling the class has been assessed as per a numerical scale value of medium, high, and low [7]. A range of regression approaches has been applied to produce a transfer function that predicts numerical values of fertility indices at the village level. The fertility soil dataset of India was made available at the block level and district level. Such datasets are suitable for decision-making about a precise quantity usage of fertilizers, the change in fertility level, and consumption depending on the fertilizer distribution process [8]. The goal is to differentiate region-wise soil nutrient fertility indices depending upon fertility datasets. [9]. This study would improve the level of

fertility in soil, thus importance of study to categorize soil nutrients like phosphorous (P), boron (B), potassium (K), and organic carbon (OC) [10]. The interest in evaluating soil parameter level with the use of the ML method helps in diminishing unwanted expenses on analysis of soil health & fertilizer input.

The paper comprises with the following: Section 2 provides related works of soil nutrient analysis. Section 3 provides proposed working of the nutrient classification system, while Section 4 displays experimental analysis. Finally, section 5 provides conclusion of the work.

II. RELATED WORK

Several works have been proposed by the researchers in the classification of soils. Zhong et al. [11] sightseen the modeling potentiality of DCNN for soil property depends on a large soil spectral library. The Land Use or Cover Area Frame Survey (LUCAS) provides the European topsoil data that has been utilized for DCNN modeling. DCNN with two single-task 16-layer methods (LucasVGGNet-16 and LucasResNet-16) have been exploited. In [12-33], presented an approach called DL for categorizing any size in particular classes. Thus, to provide multiple images, stereo-pair images have been utilized. In this study, various NN methods in DL, and a CNN have been applied to work on images. Arbawa and Dewi [13] introduced the categorization of soil nutrient content has been executed utilizing soil imagery as a substitute for laboratory soil testing.

In [14], assessed and developed CNNs, a type of DL approach to forecast properties of soil from soil spectra. The author indicated the soil spectral dataset as a 2-D spectrogram. To forecast 6 soil parameters in one method (total N, OC, clay, CEC, sand, and pH), the author proved the capability of setting multi-tasking CNNs that should be trained. Padmapriya and Sasilatha [15] introduce a multiclass soil classification utilizing ML and DL methods for the suitable determination of the soil category. The DL models VGG16, RNN, GRU, and also LSTM, SVM, and KNN, are executed and the acquired outcomes are tabulated. Akca and Gungor [16] inspected the soil salinity issue in Plain Harran, a large agricultural zone utilizing a DL-oriented U-NET system. Diverse combinations of the Salinity Index, the normalized Difference in Salinity Index, and the RapidEye multispectral images combined with Normalized Difference Vegetation Index (NDVI) to raise accuracy in segmentation.

In [17], devised a DL-oriented approach for wavelength screening in STN characteristics utilizing publicly available data named LUCAS Soil. Firstly, a network of convolution

multi-channel combined Inception method has been chosen as the benchmark method for STN forecast due to superior performance compared to other methods. Kalyani and Kolla [18] executed DL with a method utilizing a NN. NN was utilized for assessing relations between variables of 3D coordinates resulting in parameters and soil classification. Therefore, ANN is a potential tool for classifying soil. This study concentrated on the AI method utilized for predicting soil nutrient type and discussed its benefits.

Gulhane et al. [19] examine nutrients of soil study by regression process and its spectral indexed dependent upon forecast method by Iterative Self-Organizing (ISO) cluster unsupervised classifier technique. In [20], the authors intended to cloud the environment for an inversion study of salinity, moisture, nutrient content, and other essential quality indicators of soil. Dong et al. [21] the authors chose 3 vegetation restoration kinds of shrublands (SL), grasslands (GL), and forestlands (FL) along 5 slope positions for investigating the importance in restoring vegetation on soil nutrients and erodibility. Koresh & Deva [22] propose to obtain maximum productivity from the soil context and understand the ecological impact of resource data, soil functionality, and productivity function. In [23], the soil test report values can be utilized for classifying more important soil features such as village-wise soil fertility indices. Suleymanov et al. [24] concentrated on digital soil mapping (DSM) the major soil agro-chemical properties. This technique multiple linear regressions (MLR) and SVM are utilized for forecasting soil nutrients spatial distribution and difference.

III. THE PROPOSED MODEL

In this study, a new novel approach ODCNNF-STC was suggested for identifying various soil nutrients. It examines input soil images using DL models to classify them into different kinds of soil nutrients. In the ODCNNF-STC technique, several stages of operations are encompassed namely preprocessing, fusion-based feature extraction, and classification as illustrated in Fig.1.

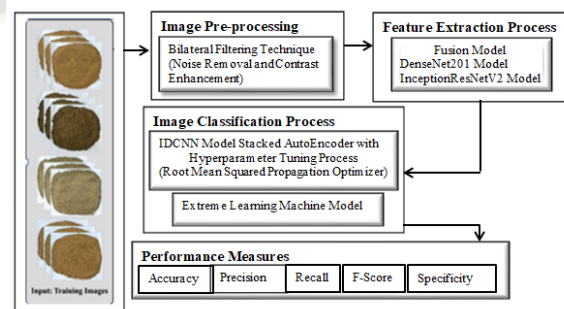


Fig. 1. Proposed ODCNNF-STC algorithm for soil nutrient classification

1. Image Preprocessing

At the preliminary stage, the images are preprocessed in two distinct ways: Bilateral Filtering noise elimination and contrast enhancement using CLAHE. The bilateral filtering makes use of nonlinear image denoising [25, 34, 35]. The linear principles of spatial Gaussian convolution that considers weighted factors for smoothing images. The principles of Gaussian convolution were demonstrated using the relation

$$g[i, j] = \frac{1}{W_{sb}} \sum_m \sum_n f[m, n] G[i - m, j - n] \quad (1)$$

Here g represents the outcome of convolution, G denotes the Gaussian spatial convolution, f shows the initial pixel value, and W_{sb} indicates the normalization factor. Gaussian convolution weights pixel of kernel by weighted Gaussian distribution equally. The bilateral filter in the proposed work can be modified as,

$$g[i, j] = \frac{1}{W_{sb}} \sum_m \sum_n f[m, n] G_{\sigma_d}[i - m, j - n] G_{\sigma_r}(f[m, n] - f[i, j]) \quad (2)$$

Where G_{σ_r} denotes the Gaussian intensity and G_{σ_d} indicates the Gaussian spatial convolution. In this work, a biased Gaussian spatial convolution with weight intensity was derived from pixels adjacent of kernels. This provides a nonlinear nature of an image with noise reduction while retaining edges. Then, the CLAHE is used to enhance contrast level of resultant image.

2. Feature Extraction using Fusion-based Models

After preprocessed, input images are used with fused two DL models to derive feature vectors. Here, the two models namely DenseNet201 and InceptionResNetV2 takes place for feature extraction. The entropy-based feature fusion procedure includes the following steps:

- i. Feature Normalization: The feature abstracted was normalized to ensure that every attribute has equal weights in the process of fusion.
- ii. Feature Extraction: Different features such as edges, corners, color gradients, shapes, textures, and object parts were mined from the input utilizing different intensity state levels that the pixel adapts.
- iii. Feature Fusion: The weighted feature was merged into a single feature vector utilizing weighted sum & fusion algorithms.
- iv. Feature Weighting: Every feature is allotted a weight depending on the entropy values to be measured by the quantity of data in the feature. In the process of fusion, features having high entropy values provide higher weights.

a) DenseNet201 Model

DenseNet201, as a CNN with a deep layer, decreases the gradient disappearance and enhances the feature efficacy and propagation, which also decreases the number of network parameters [26]. The DenseNet201 architecture connects directly each layer and makes complete communication between layers. The sub-modules of architecture is mostly transition and dense block layer. Based on the DenseNet201 architecture, if it has L layers in the DenseNet201 architecture, then there would be $L(L + 1)/2$ connection. All the input layers are derived from each preceding output layer. Let X_0 denotes the input of the entire CNN. Thus, compared to other classical CNNs namely ResNet network that relies on the final layers feature output of DenseNet201 could fuse to apply multiple lower-level extracted features, thus enhancing efficacy in utilization of features.

b) InceptionResNetV2 Model

The CNN Inception ResNetV2 [27] was trained using more than a million image from ImageNet collection. This network can group images into thousand different types of objects.

Consequently, the network picks up a lot of rich feature representations for categorizing images. It provides an input image of 299 by 299 pixels, and it produces a output list of predictive class. The residual connection and inception structure were combined into each other to create foundation of formula. The Inception-ResNet generated by combining convolution kernels with dissimilar sizes of residual connection. Once the residual connection is applied, it is likely be circumvented. Although the deep structure causes problems with degradation, it is expected to result in less time spent training. It provides a fundamental network structure that works on Inception-ResNetV2 with its iteration. This structure enhanced utilizing images of 1200 through 30 epochs at a rate of learning 0.9 SGD momentum and 0.0001 per image.

3. Image Classification

Finally, the classification of soil nutrients is performed by three classifiers namely ELM, 1DCNN with RMSProp optimizer, and SAE with RMSProp optimizer. RMSProp is a popular optimization algorithm commonly used in deep learning. It is specifically designed to address some limitations of other optimization algorithms like Stochastic Gradient Descent (SGD) and Adagrad. RMSProp adapts the learning rate for each parameter individually based on the magnitude of the recent gradients. It uses a moving average of the squared gradients to adjust the learning rate. This adaptive learning rate allows for faster convergence and improved performance by automatically adjusting the learning rate for each parameter.

a) ELM Model

ANN model has made it possible to capture intricate relations between its dependent variables and objective function [28]. This model consists of multi-layer neurons making the connections between outputs and inputs.

The outputs of all layers are weight & bias functions present in neurons processed with activation function, which is then transferred to the next layers to reach final layer. The related variables and main function provides the required neurons to input and its output layers. The hidden number (HLs) of layers and respective amount of neurons in all HLs should be specified to comprehend the construction of ANN. Furthermore, the neurons' weight and bias variables should be evaluated by performing the training model. In the process of supervised learning, initially, a series of parameters randomly are allocated to ANN variables. Next, every parameter set was predictable to the respective output value.

The original objective values were compared with the attained output value; the cost function was evaluated, which provides a modified cost function that minimalizes the neuron's weight and bias. To modify ANN neuron parameters, iterative approaches, namely gradient descent or Bayesian theorem, tend to be regarded. However, this method suffers from the slower rate of convergence for larger datasets, or evaluated solutions trapped in local minimum. The author presented the ELM which is a NN with the single HL to compass a solution. This method is selected since it is capable of generating considerably faster performance than the trained network through the BP model and it easily outperforms approaches including support vector machine, for example, regression-type application. To create the ELM, initially, a series of random numbers are allotted to the weight and bias neuron in the HL

$$\varphi_i = \sum_{j=1}^k u_k \cdot \Psi(w_j \cdot p_i + \lambda_j) \quad (3)$$

b) 1DCNN Model with RMSProp optimizer

In the 1DCNN, the convolution and pooling layers are exploited, where all convolution layers are encompassed by different convolution sizes, and the convolution kernels in the similar layer have a similar size [29]. The pooling layer adopted the average-pooling algorithm; next, the FC layer classifies the outcomes. The 1DCNN implements the convolution operations on the local region of the input signal for generating respective 1D-feature maps, and dissimilar features extracted from the input signal using convolutional kernels. All convolution kernels identify certain features at each location on the input attribute maps, to attain weight-sharing on similar input feature maps. The amount of training parameters and complexity of network is efficiently decreased due to the characteristics of weight-sharing & local

connectivity.

$$x_j^l = f \left(\sum_{i=1}^M x_i^{l-1} * k_{ij}^l + b_j^l \right) \quad (4)$$

Here * represents the convolution operator. k Indicates the convolutional kernels, j represents number of kernels, M specifies number of input channels x^{l-1} , while b designates the bias equivalent to kernel, and $f(\cdot)$ shows activation function.

The amount of feature maps rises, leading to an increase in data dimensionality that is not advantageous to computation. Thus, avg or max pooling technique is applied on all feature maps. Average pooling evaluates depends on size of predefined pooling window, and model maximal pooling chooses the maximal parameter within the range of predefined window as an output value. The FC layer of the neuron node was interconnected to each neuron node in feature map output from the prior layer, and the activation function represents the softmax function. When the last pooling layer is $l + 1$ and its output is provided to the FC layer:

$$h(x) = f(w^{l+1} \cdot x^{l+1} + b^{l+1}) \quad (5)$$

Here w indicates weight and b shows bias. In this study, the RMSProp optimizer is exploited for tuning the parameter of the 1DCNN model. The root mean squared propagation RMSProp optimizer was equivalent to SGDM optimizer [30]. The objective is to attenuate oscillation similar to momentum. Also, it removes the necessity to automatically adapt to the learning rate by doing so. Furthermore, it chooses a discrete learning rate for all the parameters. Also, note that RMSProp carries out simulated annealing by default. RMSProp decreases size in gradient steps toward minima for larger steps.

c) SAE Model with RMSProp optimizer

Autoencoder (AE) is a DL-architecture recreates at the output the original signal received at input by going through an intermediate layer having the minimum amount of nodes hidden. It learns abstract and deep features in the decreased hidden nodes [31]; hence, the reconstruction can be possible from them. Where the input signal $p \in \mathcal{R}^N$ is decreased to F features presenting higher abstraction, and lastly, the original signal reconstructed into $z \in \mathcal{R}^N$. The training of AE includes regenerating input signal at output, hence internal unit is capable of providing the original data. The value in the layer is applied as a new feature presenting the original signal p .

$$y = f(w_y p + b_y) \quad , \quad z = f(w_z y + b_z) \quad (6)$$

Here, the interval parameter $y \in \mathcal{R}^F$ is attained from p through the weights w_y and bias b_y and reconstruction signal $z \in \mathcal{R}^N$, expected to match p , is attained from layer output y by w_z and b_z ; f denotes the activation function that

presents the non-linearity in the model. The error between p and z needs to be decreased for training the AE and defining the optimized parameters.

$$\Omega = \arg \min_{w_y, w_z, b_y, b_z} [\text{error}(p, z)] \quad (7)$$

SAEs are determined by extending these concepts and simply presenting different layers between the output and the input. Thus, the final feature was attained by progressive abstraction level. A SAE with 2 layers was demonstrated, where generally $F < L$.

In hyper spectral remote sensing, SAEs are exploited for reduction in feature of pixels in spectral field, in unsupervised way. Afterward, SAE is trained with part of the samples, all the pixels are decreased to output value (y) of deep layer. The training of SAEs includes an iterative updating of w and b internal coefficients an update through error between the input pixels and reconstruction once the network output was gradually decreased or threshold. The similarity between both profiles is clear with the reconstructed profile and original spectral data after suitable training of SAE. This similarity shows that the SAE model was capable of reconstructing input pixels from the internal layer with the decreased amount of nodes through which features F decreased and have major data high abstraction of the pixel. To improve the efficacy of the SAE model, the RMSProp optimizer is used.

IV. RESULT AND DISCUSSION

This section examines ODCNNF-STC technique on a 110 images of soil samples gathered around the Tumkur district, Karnataka, India. The dataset represents the different soil types around rural areas of Bangalore, Karnataka, India. The samples are collected at a distance of radius of approximately 3-5 km with a depth of 1 foot in the ground. The images are captured in the size of 1280x1194 (pixels) approximately by using a compact digital camera with a potential megapixel CMOS image sensor and are saved in jpeg file format. The image dataset is uploaded to the repository Kaggle. Fig. 2 portrays the sample images.



Fig. 2. Sample Images

The soil nutrient parameters involved are Soil Reaction, Boron, Iron, Manganese, Organic Carbon, Phosphorus, Potassium, Sulphur, Copper, and Zinc. The feature map shows the features such as color, lines, texture, shapes, and context-

specific patterns. Fig. 3 represents feature maps from proposed method.

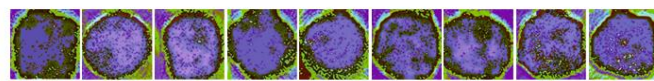


Fig. 3. Proposed Feature Extraction Model-obtained Feature Maps

Using the ELM classifier, the average accuracy in the classification of soil reaction classes, organic compound, Sulphur, Iron, and copper was estimated as 90.91%, 96.97%, 96.97%, 93.94%, and 96.97% respectively. For other classifications such as phosphorous, potassium, Manganese, and Zinc, the maximum accuracy attained. The average precision in classification of soil reaction, Organic carbon, sulphur, Iron, and Copper was estimated as 97.5%, 96.88%, 98.75%, 96.55%, and 95.45% respectively. Fig. 4 illustrates the performance comparison of the ELM classifier obtained from the test data.

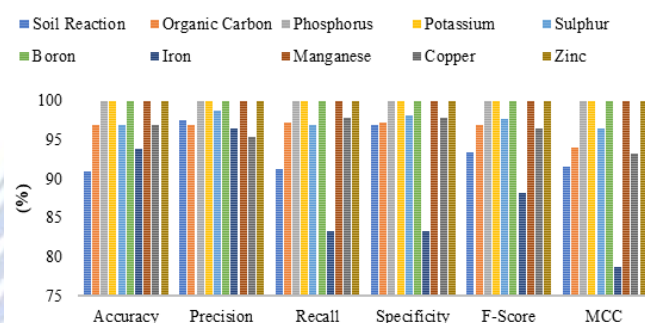


Fig. 4. Comparison of ELM classifier testing performance in different soil nutrient analysis

Fig. 5 illustrates the graphical comparison of performance obtained on the SEM classifier using the test data. The average accuracy, precision, recall, specificity, and F-score of sulphur estimated as 96.97%, 98.75%, 96.88%, 98.21%, 97.69%, and 96.41% respectively. The average accuracy and precision in the classification of Iron is estimated as 87.88% and 79.63% respectively.

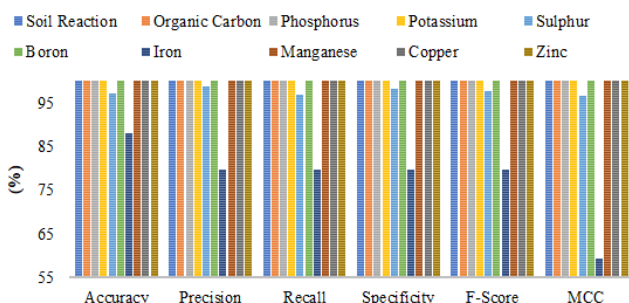


Fig. 5. Comparison of SAE classifier testing performance in different soil nutrient analysis

Fig. 6 illustrates the graphical comparison of performance obtained using the 1D-CNN classifier. The percentage of accuracy, precision, recall, specificity, F-score, and MCC in

classification of phosphorous was estimated as 96.97%, 98.55%, 96.3%, 96.97%, 97.3%, and 95.21% respectively. Similarly in the classification of potassium, the 1D-CNN classifier yields an accuracy, precision, recall, specificity, F-score, and MCC of 96.97%, 91.67%, 98.85%, 98.89%, 94.65%, and 91.01% respectively. The maximum performance is attained for other soil nutrient classifications as illustrated in Fig. 6.

Table 1 illustrates the comparison of three models average performance in both training and testing. The average testing accuracy in the ELM and SAE classifier was estimated as 97.58% and 98.49% respectively which is 0.67% and 0.31% lower than the training accuracy. In the case of 1D-CNN, the average testing accuracy was 0.72% higher than its training accuracy. The 1D-CNN architecture results in a testing accuracy, precision, recall, specificity, F-score, and MCC of 99.39%, 99.02%, 99.52%, 99.59%, 99.52% and 98.62% respectively.

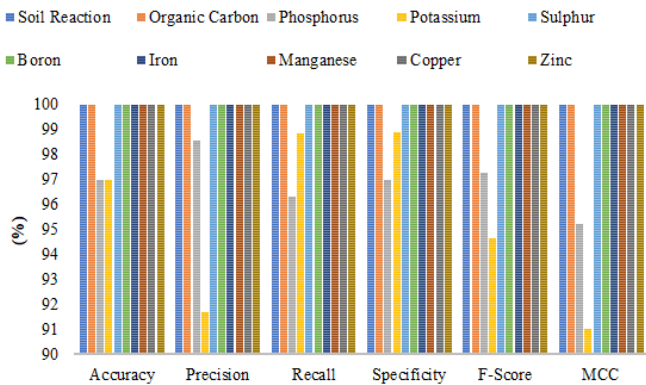


Fig. 6. Comparison of 1D-CNN classifier testing performance in different soil nutrient analysis

Table 1 Comparison of performance of the models ELM, SAE, and 1D-CNN during training and Testing

Classifiers		Accuracy (%)	Precision (%)	Recall (%)	Specificity (%)	F-Score (%)	MCC (%)
Training	ELM	98.27	98.04	97.79	98.03	97.86	96.07
	SAE	98.8	99.11	97.21	97.6	97.97	96.47
	1-DCNN	98.67	98.74	97.43	98.6	98.01	97.05
Testing	ELM	97.58	98.51	96.65	97.35	97.27	95.42
	SAE	98.49	97.84	97.65	97.78	97.73	95.57
	1-DCNN	99.39	99.02	99.52	99.59	99.2	98.62

The confusion matrices obtained for the 1D-CNN model on test images are provided in Fig. 7. It resembles the number

of classes in each Category. In each category class 0 resembles the category of lower concentration, while class N resembles the category of higher concentration. For example in the case of soil reaction, class 0 resembles the presence of a lower soil reaction, while class 5 resembles the presence of a higher soil reaction. Classes 1, 2, 3, and 4 resemble the soil reaction between 0 and 5 classes. The classification result provided in the confusion matrix shows proposed ODCNN-STC model provides better classification result.

Fig. 8 exhibits the ROC curve analysis of the ELM, SAE, and 1DCNN classifier models. The ROC curve attained by the 1DCNN model is found to have a higher AUC characteristic than the other ELM and SAE classifier models. The average AUC for the models' ELM, SAE, and 1D-CNN was estimated as 0.9891, 0.9894, and 0.9915 respectively.

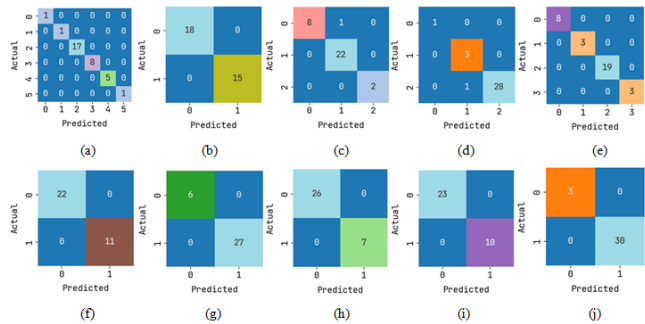


Fig. 7. Confusion Matrix on Testing Set for 1D-CNN (a) Soil reaction (b) Organic carbon (c) Phosphorous (d) Potassium (e) Sulphur (f) Boron (g) Iron (h) Manganese (i) Copper (j) Zinc

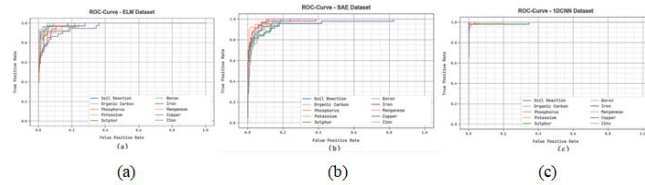


Fig. 8. ROC analysis - three classifiers used in the proposed method (a) ELM classifier (b) SAE classifier (c) 1D-CNN classifier

Table 2 Performance comparison of proposed work with other recent classifiers [32]

Methods	Accuracy (%)	Precision (%)	Recall (%)	Specificity (%)	F-Score (%)
RF Model	97.94	95.31	98.16	93.26	98.34
NB Model	98.65	96.52	95.76	94.24	96.91
SVM Model	98.7	97.24	94.62	96.92	97.58
DT Model	98.44	96.21	98.32	94.26	96.97
LS-SVM Model	97.57	97.14	95.78	97.21	95.34

ANN Model	97.9	98.12	97.34	96.12	95.38
Gaussian RBF	98.83	97.43	96.24	98.16	97.34
Proposed	99.39	99.02	99.52	99.59	99.2

The Table 2 shows performance of proposed ODCNNF-STC was compared with traditional classifiers[32] such as least squares-SVM ,Random forest (RF), decision tree (DT), Naïve Bayes (NB), Support vector machine (SVM), Artificial neural network (ANN) and Gaussian radial basis function (RBF). The classifiers NB, SVM, DT, and Gaussian RBF models have accomplished closer accuracy values of 98.65%, 98.70%, 98.44%, and 98.83% respectively. Nevertheless, the ODCNNF-STC technique exhibits superior results with an increased accuracy of 99.39%. The proposed approach has an increase in accuracy of 0.56% than the Gaussian RBF model.

In Fig. 9 the performance of proposed method with traditional classifiers were illustrated in graphical representation. In comparison to conventional approaches, the proposed approach performs better in terms of accuracy, precision, recall, specificity, and F-Score.

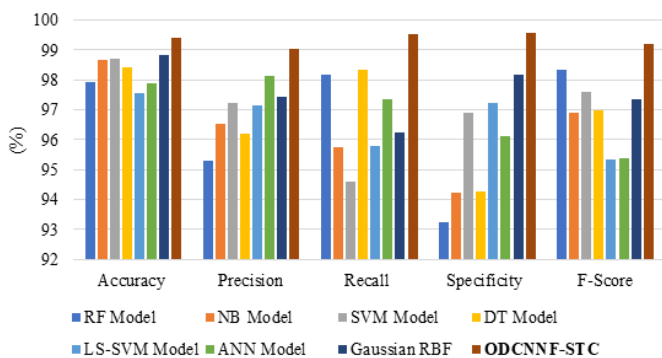


Fig. 9. Performance comparison of ODCNNF-STC approach with traditional schemes

V. CONCLUSION

This novel technique ODCNNF-STC was introduced for soil nutrients classification. It examines the input soil images using DL models to classify them into different kinds of soil nutrients. In the ODCNNF-STC technique, several stages of operations are encompassed namely preprocessing, fusion-based feature extraction, and classification. For the extracting features a fusion of two models namely DenseNet201 and InceptionResNetV2 were used. Finally, the classification of soil nutrients is performed by three classifiers namely ELM, 1DCNN with RMSProp optimizer, and SAE with RMSProp optimizer. The results of the ODCNNF-STC technique are examined on the real-time dataset of soil images and results exhibit better performance of ODCNNF-STC technique with other algorithms in terms of various measures. Metaheuristic

hyperparameter optimizers can improve ODCNNF-STC technique's performance in the future.

REFERENCES

- [1] Zhou, C., Hu, J., Xu, Z., Yue, J., Ye, H. and Yang, G., 2020. A novel greenhouse-based system for the detection and plumpness assessment of strawberry using an improved deep learning technique. *Frontiers in plant science*, 11, p.559.
- [2] Janani, M. and Jebakumar, R., 2023. Detection and classification of groundnut leaf nutrient level extraction in RGB images. *Advances in Engineering Software*, 175, p.103320.
- [3] Riese, F.M. and Keller, S., 2019. Soil texture classification with 1D convolutional neural networks based on hyperspectral data. *arXiv preprint arXiv:1901.04846*.
- [4] Palaparthi, A., Ramiya, A.M., Ram, H. and Mishra, D., 2023, January. Classification of Horticultural Crops in High Resolution Multispectral Imagery Using Deep Learning Approaches. In *2023 International Conference on Machine Intelligence for GeoAnalytics and Remote Sensing (MIGARS) (Vol. 1, pp. 1-4)*. IEEE.
- [5] Lanjewar, M.G. and Gurav, O.L., 2022. Convolutional Neural Networks based classifications of soil images. *Multimedia Tools and Applications*, 81(7), pp.10313-10336.
- [6] İnik, O., İnik, Ö., Öztas, T., Demir, Y. and Yüksel, A., 2023. Prediction of Soil Organic Matter with Deep Learning. *Arabian Journal for Science and Engineering*, pp.1-21.
- [7] Nasiri, A., Omid, M., Taheri-Garavand, A. and Jafari, A., 2022. Deep learning-based precision agriculture through weed recognition in sugar beet fields. *Sustainable Computing: Informatics and Systems*, 35, p.100759.
- [8] Odebiri, O., Mutanga, O., Odindi, J. and Naicker, R., 2023. Mapping soil organic carbon distribution across South Africa's major biomes using remote sensing-topo-climatic covariates and Concrete Autoencoder-Deep neural networks. *Science of The Total Environment*, 865, p.161150.
- [9] Suhag, S., Singh, N., Jadaun, S., Johri, P., Shukla, A. and Parashar, N., 2021, June. IoT based soil nutrition and plant disease detection system for smart agriculture. In *2021 10th IEEE International Conference on Communication Systems and Network Technologies (CSNT) (pp. 478-483)*. IEEE.
- [10] Durai, S.K.S. and Shamili, M.D., 2022. Smart farming using machine learning and deep learning techniques. *Decision Analytics Journal*, 3, p.100041.
- [11] Zhong, L., Guo, X., Xu, Z. and Ding, M., 2021. Soil properties: Their prediction and feature extraction from the LUCAS spectral library using deep convolutional neural networks. *Geoderma*, 402, p.115366.
- [12] Azizi, A., Gilandeh, Y.A., Mesri-Gundoshmian, T., Saleh-Bigdeli, A.A. and Moghaddam, H.A., 2020. Classification of soil aggregates: A novel approach based on deep learning. *Soil and Tillage Research*, 199, p.104586.
- [13] Arbawa, Y.K. and Dewi, C., 2020. Soil Nutrient Content Classification for Essential Oil Plants using kNN.

- In Proceedings of the 2nd International Conference of Essential Oils (pp. 96-100).
- [14] Padarian, J., Minasny, B. and McBratney, A.B., 2019. Using deep learning to predict soil properties from regional spectral data. *Geoderma Regional*, 16, p.e00198.
- [15] Padmapriya, J. and Sasilatha, T., 2023. Deep learning based multi-labelled soil classification and empirical estimation toward sustainable agriculture. *Engineering Applications of Artificial Intelligence*, 119, p.105690.
- [16] Akca, S. and Gungor, O., 2022. Semantic segmentation of soil salinity using in-situ EC measurements and deep learning based U-NET architecture. *Catena*, 218, p.106529.
- [17] Wang, Y., Li, M., Ji, R., Wang, M. and Zheng, L., 2021. A deep learning-based method for screening soil total nitrogen characteristic wavelengths. *Computers and Electronics in Agriculture*, 187, p.106228.
- [18] Kalyani, N.L. and Kolla, B.P., 2022. Soil Color as a Measurement for Estimation of Fertility using Deep Learning Techniques. *International Journal of Advanced Computer Science and Applications*, 13(5).
- [19] Gulhane, V.A., Rode, S.V. and Pande, C.B., 2023. Correlation analysis of soil nutrients and prediction model through ISO cluster unsupervised classification with multispectral data. *Multimedia Tools and Applications*, 82(2), pp.2165-2184.
- [20] Zhang, T., Zhang, Y., Wang, A., Wang, R., Chen, H. and Liu, P., 2023. Intelligent Analysis Cloud Platform for Soil Moisture-Nutrients-Salinity Content Based on Quantitative Remote Sensing. *Atmosphere*, 14(1), p.23.
- [21] Dong, L., Li, J., Zhang, Y., Bing, M., Liu, Y., Wu, J., Hai, X., Li, A., Wang, K., Wu, P. and Shanguan, Z., 2022. Effects of vegetation restoration types on soil nutrients and soil erodibility regulated by slope positions on the Loess Plateau. *Journal of Environmental Management*, 302, p.113985.
- [22] Koresh, M.H. and Deva, J., 2021. Analysis of soil nutrients based on potential productivity tests with balanced minerals for maize-chickpea crop. *J. Electron*, 3(01), pp.23-35.
- [23] Suchithra, M.S. and Pai, M.L., 2020. Improving the prediction accuracy of soil nutrient classification by optimizing extreme learning machine parameters. *Information processing in Agriculture*, 7(1), pp.72-82.
- [24] Suleymanov, A., Abakumov, E., Suleymanov, R., Gabbasova, I. and Komissarov, M., 2021. The soil nutrient digital mapping for precision agriculture cases in the trans-ural steppe zone of Russia using topographic attributes. *ISPRS International Journal of Geo-Information*, 10(4), p.243.
- [25] Anam, C., Naufal, A., Sutanto, H., Adi, K. and Dougherty, G., 2022. Impact of Iterative Bilateral Filtering on the Noise Power Spectrum of Computed Tomography Images. *Algorithms*, 15(10), p.374.
- [26] Zhou, Z., Liu, M., Deng, W., Wang, Y. and Zhu, Z., 2023. Clothing Image Classification with DenseNet201 Network and Optimized Regularized Random Vector Functional Link. *Journal of Natural Fibers*, 20(1), p.2190188.
- [27] Karanam, S.R., Srinivas, Y. and Chakravarty, S., 2023. A Supervised Approach to Musculoskeletal Imaging Fracture Detection and Classification Using Deep Learning Algorithms. *Computer Assisted Methods in Engineering and Science*.
- [28] Forootan, E., Dehvari, M., Farzaneh, S. and Karimi, S., 2023. Improving the Wet Refractivity Estimation Using the Extremely Learning Machine (ELM) Technique. *Atmosphere*, 14(1), p.112.
- [29] Huang, S., Tang, J., Dai, J. and Wang, Y., 2019. Signal status recognition based on 1DCNN and its feature extraction mechanism analysis. *Sensors*, 19(9), p.2018.
- [30] Fakhry, M. and Brery, A.F., 2022, March. A comparison study on training optimization algorithms in the biLSTM neural network for classification of PCG signals. In *2022 2nd International Conference on Innovative Research in Applied Science, Engineering and Technology (IRASET)* (pp. 1-6). IEEE.
- [31] Zabalza, J., Ren, J., Zheng, J., Zhao, H., Qing, C., Yang, Z., Du, P. and Marshall, S., 2016. Novel segmented stacked autoencoder for effective dimensionality reduction and feature extraction in hyperspectral imaging. *Neurocomputing*, 185, pp.1-10.
- [32] Trontelj ml., J.; Chambers, O. Machine Learning Strategy for Soil Nutrients Prediction Using Spectroscopic Method. *Sensors* 2021, 21, 4208. <https://doi.org/10.3390/s21124208>.
- [33] G. Sharmila and K. Rajamohan, "Soil classification using active contour model for efficient texture feature extraction," *Int. J. Inf. Technol.*, vol. 15, no. 7, pp. 3791–3805, 2023, doi: 10.1007/s41870-023-01404-6.
- [34] G. Sharmila and K. Rajamohan, "Image Processing and Artificial Intelligence for Precision Agriculture," *Proc. 2022 Int. Conf. Innov. Comput. Intell. Commun. Smart Electr. Syst. ICSES 2022*, pp. 1–8, 2022, doi: 10.1109/ICSES55317.2022.9914148.
- [35] G. Sharmila and K. Rajamohan, A Systematic Literature Review on Image Preprocessing and Feature Extraction Techniques in Precision Agriculture, vol. 114. Springer Nature Singapore, 2022.